JTTEE5 9:494-498

Formation of Amorphous Fe-Cr-Mo-8P-2C Coatings by the High Velocity Oxy-Fuel Process

F. Otsubo, H. Era, and K. Kishitake

(Submitted 1 July 1999)

Alloy powders of Fe-10%Cr-8%P-2%C(10Cr), Fe-20%Cr-8%P-2%C(20Cr), and Fe-10%Cr-10%Mo-8%P-2%C(10Mo) compositions (in mass%) were sprayed by the high velocity oxy-fuel (HVOF) process under different conditions. The as-sprayed coatings of 10Mo alloy were composed of only an amorphous phase under all the spray conditions, while the as-sprayed coatings of the 10Cr and 20Cr alloys consisted of an amorphous phase with a small amount of crystalline material. The volume fraction of the crystalline material increased slightly with the rise of the flame temperature. The hardnesses of the as-sprayed coatings of the 10Cr and 20Cr alloys were 600 to 700 DPN, respectively, while the 10Mo coating composed of an amorphous phase revealed 560 DPN. The corrosion resistance of the as-sprayed coating of the 10Mo alloy was the best among three amorphous coatings and also superior to the nickel-base self-fluxing alloy and SUS316L stainless steel coatings in 1*N* H_2SO_4 and 1*N* HCl solutions.

Keywords amorphous coating, corrosion resistance, HVOF, iron alloy, structure

1. Introduction

Previous work[1] has reported on the structure and corrosion resistance of Fe-10at.%Cr-13at.%P-7at.%C amorphous coatings obtained by low-pressure plasma spraying (LPPS), high-energy plasma spraying (HPS), and high velocity oxy-fuel (HVOF) processes. It was found that a 100% amorphous coating was formed only by the LPPS process, and the corrosion resistance of the coating was excellent in sulfuric acid and hydrochloric acid solutions.

The LPPS process is not practical for all industrial processes due to the need to process in a low-pressure vessel. An amorphous coating was also formed by HPS and HVOF processes under atmospheric conditions, but these coatings also included crystalline phases. A 100% amorphous coating has not been obtained with thermal spray processes under atmospheric conditions. The flame temperature of the HVOF process is low and the flame speed is very high compared with a plasma spraying process. Therefore, it is anticipated that a 100% amorphous coating would be formed by the HVOF process under atmospheric conditions by using alloy powders, which had a tendency to form an amorphous phase.

Hashimoto *et al.* reported[2,3,4] that the addition of molybdenum and/or tungsten to Fe-Cr-P-C alloy enhances the corrosion resistance of the amorphous alloys. It is also known that the addition of molybdenum increases the amorphous forming ability of high carbon iron alloys.[5,6] Accordingly, an amorphous coating without crystalline phases could be formed by the HVOF process by using appropriate powders, and the corrosion resistance of the coating would be better than the amorphous coating of the Fe-Cr-P-C alloy.

The aim of this work is to form a 100% amorphous iron-based coating by the HVOF process under atmospheric conditions and to investigate the corrosion resistance of the coating.

F. Otsubo, H. Era, and **K. Kishitake,** Department of Materials Science and Engineering, Faculty of Engineering, Kyushu Institute of Technology, Kita-Kyushu 804-8550, Japan. Contact e-mail: otsubo@tobata.isc.kyutech.ac.jp.

2. Experimental Procedure

The iron alloy powders were made by gas atomization after melting electrolytic iron, graphite, and ferroalloys by using an induction furnace. The chemical compositions of the alloy powders are shown in Table 1. The compositions of the powders are similar to the high corrosion-resistant amorphous alloys of Fe-Cr-Mo-13at.%P-7at.%C reported by Hashimoto *et al.*[2] The 10Cr alloy is the same as the Fe-10.9Cr-13.1P-8.36C-0.77Si (at.%) alloy investigated in the previous paper.[1] A small amount of silicon was added to prevent oxidation through the atomization process.

Alloy powders of 45 to 10 μm in diameter were used for spraying. The alloy powders are of an amorphous phase, as seen from the x-ray diffraction (XRD) patterns in Fig. 1. The melting point of the powders is under 1273 K, as shown in Table 2.

The powders were sprayed onto a mild steel plate by the HVOF process under the three different conditions shown in Table 3. The oxygen and fuel pressures of the HVOF process were changed to vary the flame temperature. The thickness of the coatings obtained was about 0.5 mm. The structure and phases in the coatings were examined by XRD and optical microscopy. The hardness of the coatings was measured 15 times using a Vickers microhardness tester with a 4.9 N load. The corrosion resistance of the coatings was evaluated from anodic polarization curves in acidic solutions using a potentiostat. De-aerated 1*N* H_2SO_4 and 1*N* HCl solutions were used for the electrolyte. A platinum counterelectrode and a saturated calomel reference electrode (SCE) were used. The anodic polarization curves of the coatings were obtained by scanning the corrosion potential to +1.1 V (versus SCE) with a scanning rate of 60 mV/min after keeping the potential at −0.7 V (versus SCE) for 10 min at 303

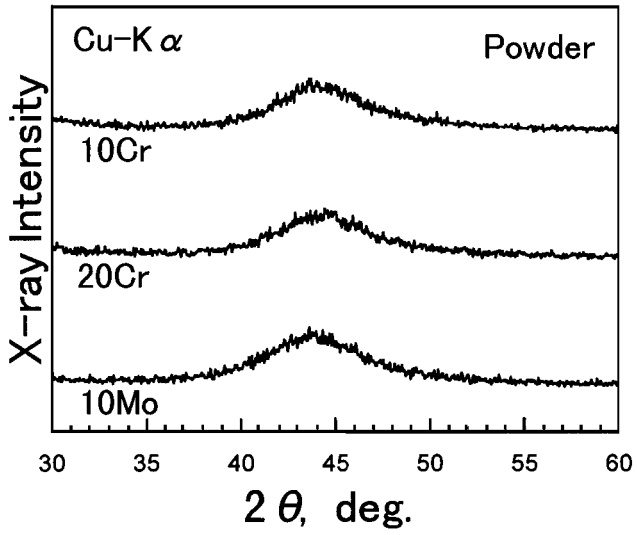

Fig. 1 XRD patterns of powders

Table 1 Chemical compositions of powders (mass%)

Alloy	Cr	Mo	P	C	Si
10Cr	11.7	. . .	8.36	2.08	0.46
20Cr	19.9	. . .	8.13	2.07	0.46
10Mo	10.0	11.7	7.69	2.11	0.65

Table 2 Melting point of alloys (K)(a)

10Cr	20Cr	10Mo
1237	1271	1218

(a) Measured on heating rate of 0.5 K/s

Table 3 HVOF spraying conditions

	Condition		
	L	M	H
Oxygen pressure, MPa	1.275	1.241	1.206
Fuel pressure, MPa	0.931	0.965	0.965
Chamber pressure, MPa	0.689	0.689	0.689
Feed rate, g/min	45	45	45
Spray distance, mm	300	300	300

K. The coatings were polished with alumina powders of 0.05 μm and were masked with an acid-resistant lacquer to form an exposure area of 1 cm^2 before the measurement of the anodic polarization curve.

3. Results and Discussion

3.1 Structure of Coating

The temperature of the substrate heated by the HVOF flame was measured by means of a thermocouple welded at a distance of 1 mm between each wire of the thermocouple on the center of

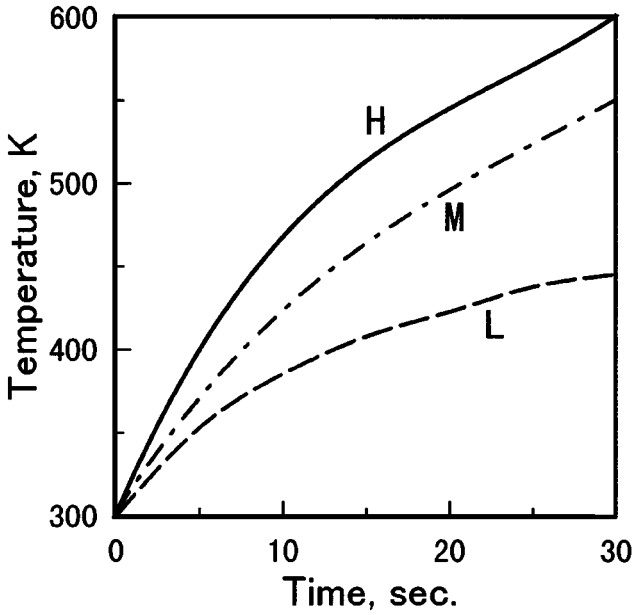

Fig. 2 Temperature change of substrate heated by HVOF flame

a steel plate ($3^t \times 50 \times 60$ mm). Figure 2 shows the temperature change of the plate as a function of the spray time without the powder feeding. The temperature elevates more quickly in the order of conditions L, M, and H.

Figure 3 shows optical micrographs of the as-sprayed coatings of 10Cr alloy. The coatings appear very dense, although some pores and oxide films are visible in the coatings. The pore size in the coating sprayed under the condition of L is larger than that in the coating sprayed under condition H. The 20Cr and 10Mo coatings also exhibited similar structures as the 10Cr coating sprayed under the same condition.

Figure 4 shows the XRD patterns of the as-sprayed coatings of 10Cr alloy. Very weak diffraction peaks are seen on a halo pattern in the coating sprayed under condition L. The peaks become more distinct for coatings sprayed under conditions M and H. Figure 5 shows the XRD patterns of the as-sprayed coatings of the 20Cr alloy. The peaks are more clearly distinguished on a halo pattern compared with the 10Cr coating sprayed under the same conditions. On the other hand, the XRD patterns of the as-sprayed coatings of the 10Mo alloy reveal a halo pattern without any peaks of crystal phases under all conditions (Fig. 6). It is found that the 10Mo alloy is the best feedstock to use to achieve an amorphous coating by the HVOF process.

Figure 7 shows the hardness of the as-sprayed coatings. The 10Cr and 20Cr coatings revealed high hardnesses of 600 to 700 DPN, and the hardness increases in the order of the conditions L, M, and H because of the increase in the volume fraction of crystalline phases in this order. On the other hand, the 10Mo coatings composed of a perfect amorphous phase show similar hardnesses of 560 DPN independently of the spray condition.

3.2 Corrosion Resistance

Anodic polarization curves of the coatings sprayed under condition L were measured in acidic solutions. Figure 8 shows

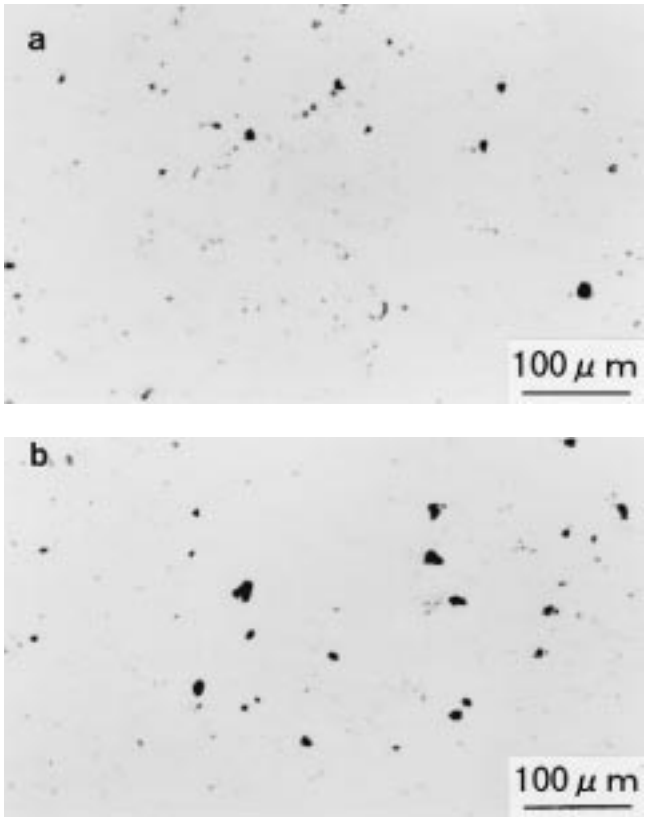

Fig. 3 Optical micrographs of the coatings of 10Cr alloy sprayed under the conditions of (**a**) H and (**b**) L

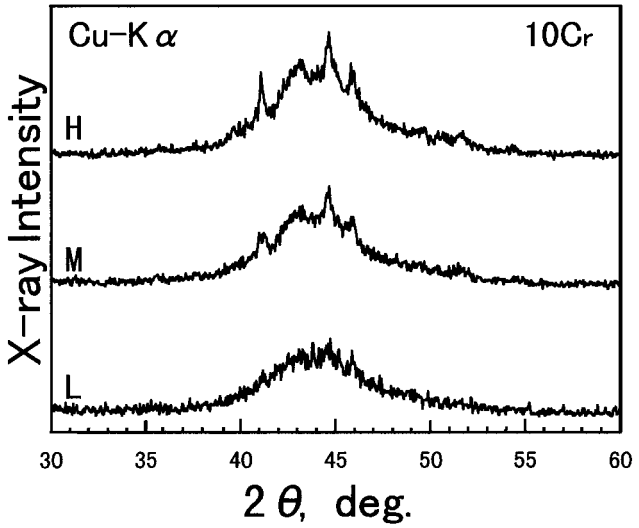

Fig. 4 XRD patterns of as-sprayed coating of 10Cr alloy

anodic polarization curves of the as-sprayed coatings in de-aerated 1*N* H_2SO_4 solution at 303 K. The polarization curves of nickel-base self-fluxing alloy (SFA) coating (JIS-MSFNi1),[7] SUS316L stainless steel coating, and Hastelloy C alloy plate are also shown for comparison. The as-sprayed coatings of the 10Cr

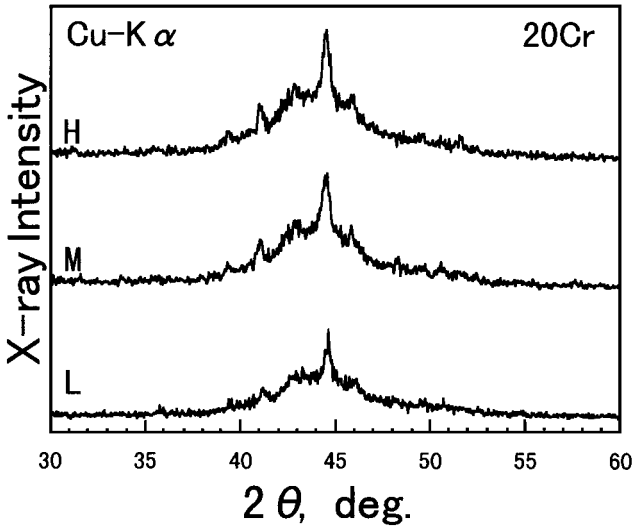

Fig. 5 XRD patterns of as-sprayed coating of 20Cr alloy

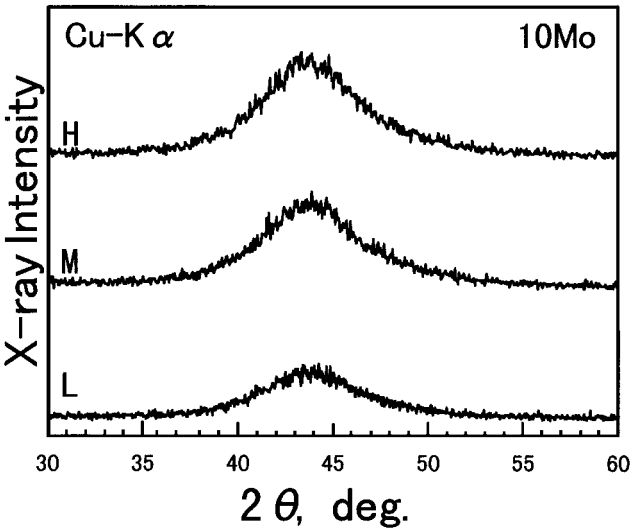

Fig. 6 XRD patterns of as-sprayed coating of 10Mo alloy

and 20Cr alloys exhibit the activation-passivation transition. However, the 10Mo alloy coating reveals the higher corrosion potential of 0.1 V compared with the other amorphous coatings and no active state in the polarization curve. The passivation current density of the 10Mo coating is the lowest among the three amorphous coatings. Therefore, the corrosion resistance of the 10Mo coating composed of a 100% amorphous phase is superior to the other partially amorphous coatings. The current densities of the SFA and SUS316L coatings are much larger than those of the amorphous coatings, and the current density of the Hastelloy C alloy plate is quite low. Accordingly, the corrosion resistance of the amorphous coatings may be superior to the SFA and SUS316L coatings and inferior to Hastelloy C plate in 1*N* H_2SO_4 solution.

Figure 9 shows anodic polarization curves of the as-sprayed coatings in de-aerated 1*N* HCl solution at 303 K. The polariza-

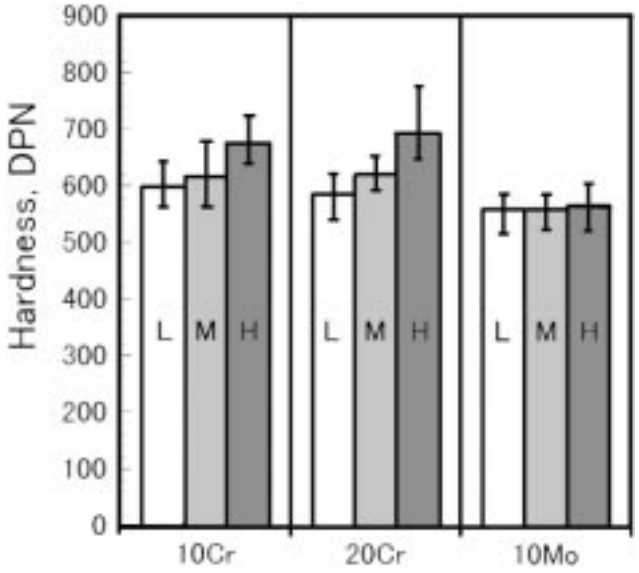

Fig. 7 Hardness of as-sprayed coatings. Longitudinal bars at the top of the rectangle show the range of maximum and minimum hardnesses

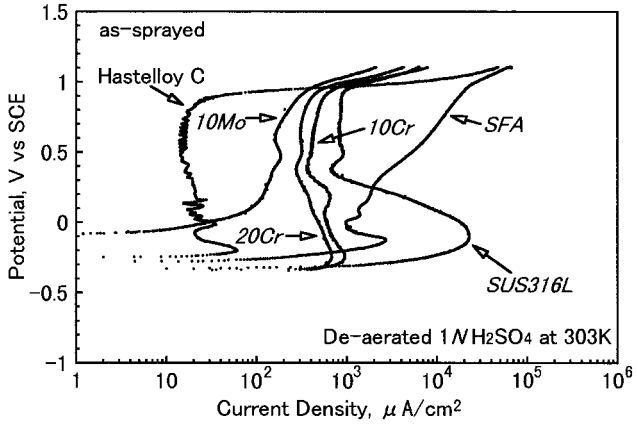

Fig. 8 Anodic polarization curves of as-sprayed coatings in 1*N* H_2SO_4 solution

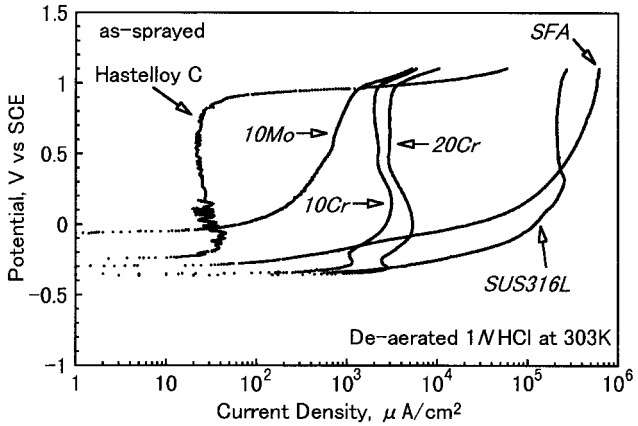

Fig. 9 Anodic polarization curves of as-sprayed coatings in 1*N* HCl solution

tion curves of the amorphous coatings in 1*N* HCl solution are similar to those of the coatings in 1*N* H_2SO_4 solution. Hastelloy C alloy, which possesses high corrosion resistance in 1*N* H_2SO_4 solution, also retains a quite low current density in 1*N* HCl solution. However, the current density of the SFA and SUS316L coatings in 1*N* HCl solution become fairly large compared with those in 1*N* H_2SO_4 solution. Therefore, the amorphous coatings possess higher corrosion resistance also in 1*N* HCl solution compared with SFA and SUS316L coatings. Thus, it was found that a 100% amorphous coating was obtained by the HVOF process under atmospheric conditions using Fe-Cr-Mo-P-C alloy powders, and the coating exhibited good corrosion resistance in 1*N* H_2SO_4 and 1*N* HCl solutions.

4. Conclusions

The Fe-10Cr-8P-2C(10Cr), Fe-20Cr-8P-2C(20Cr), and Fe-10Cr-10Mo-8P-2C(10Mo) amorphous powder compositions in mass percent were sprayed by the HVOF process under various atmospheric conditions. The structure, hardness, and corrosion resistance of the coatings were investigated. The results are summarized as follows.

- Amorphous coatings with a small amount of crystalline phases are obtained from the 10Cr and 20Cr alloys and a 100% amorphous coating is formed from the 10Mo alloy by the HVOF process.
- The volume fraction of crystalline phases in the 10Cr and 20Cr coatings increases slightly with a rise of the flame temperature. The hardnesses of the 10Cr and 20Cr coatings are 600 to 700 DPN. On the other hand, the 10Mo coatings composed of a perfect amorphous phase reveal a constant hardness of 560 DPN independently of the spray condition.
- The as-sprayed coatings of the 10Cr and 20Cr alloys exhibit the activation-passivation transition. However, the as-sprayed coating of the 10Mo alloy showed a higher corrosion potential of about 0.1 V compared with the other as-sprayed coatings and revealed no active state in anodic polarization curves in 1*N* H_2SO_4 and 1*N* HCl solutions.
- The corrosion resistance of the as-sprayed coatings is superior to the SFA and SUS316L coatings in 1*N* H_2SO_4 and 1*N* HCl solutions, and the as-sprayed coatings possess higher corrosion resistance in 1*N* HCl solution than in 1*N* H_2SO_4 solution compared with SFA and SUS316L coatings. The as-sprayed coating of the 10Mo alloy composed of a 100% amorphous phase structure has excellent corrosion resistance in 1*N* H_2SO_4 and 1*N* HCl solutions.

Acknowledgments

This research was supported by a grant-in-aid for scientific research from the Ministry of Education in Japan. The authors acknowledge the Center for Instrumental Analysis, Kyushu Institute of Technology, for XRD analysis. Also, the authors' thanks are due to Fujikikosan Corporation for preparing coatings. Mr. T. Aiko, formerly Graduate Student, Kyushu Institute

of Technology, and Messrs. A. Sameshima and N.Abe, formerly Students, Kyushu Institute of Technology, assisted with the experiment.

References

1. K. Kishitake, H. Era, and F. Otsubo: *J. Thermal Spray Technol.*, 1996, vol. 5, pp. 476-82.
2. K. Kobayashi, K. Hashimoto, and T. Masumoto: *Sci. Rep. Res. Inst. Tohoku Univ.*, 1981, vol. A29, pp. 284-95.
3. H. Habazaki, A. Kawashima, K. Asami, and K. Hashimoto: *J. Electrochem. Soc.*, 1991, vol. 138, pp. 76-81.
4. H. Habazaki, A. Kawashima, K. Asami, and K. Hashimoto: *Corr. Sci.*, 1992, vol. 33, pp. 225-36.
5. A. Inoue, T. Masumoto, S. Arakawa, and T. Iwadachi: *Trans. JIM*, 1978, vol. 19, pp. 303-04.
6. K. Kishitake, H. Era, and Ping Li: *Mater. Trans. JIM*, 1993, vol 34, pp. 54-61.
7. *Japanese Industrial Standards (JIS)*, 1994, Standard No. H 8303 (in Japanese).